Initial stages of ion beam-induced phase transformations in Gd_2O_3 and Lu_2O_3

Chien-Hung Chen,[1,a)] Cameron L. Tracy,[1] Chenxu Wang,[1] Maik Lang,[2] and Rodney C. Ewing[1]
[1]*Department of Geological Sciences, Stanford University, Stanford, California 94305, USA*
[2]*Department of Nuclear Engineering, University of Tennessee, Knoxville, Tennessee 37996, USA*

(Received 9 November 2017; accepted 29 January 2018; published online 13 February 2018)

The atomic-scale evolution of lanthanide sesquioxides Gd_2O_3 and Lu_2O_3 irradiated with 1 MeV Kr ions at room temperature and 120 K, up to fluences of 1×10^{16} ions/cm^2 (~20 dpa), has been characterized by *in situ* transmission electron microscopy. At room temperature, both oxides exhibited high radiation tolerance. Irradiation did not cause any observable structural change in either material, likely due to the mobility of irradiation-induced point defects, causing efficient defect annihilation. For Gd_2O_3, having the larger cation ionic radius of the two materials, an irradiation-induced stacking fault structure appeared at low fluences in the low temperature irradiation. As compared with the cubic-to-monoclinic phase transformations known to result from higher energy (~GeV) ion irradiation, Kr ions of lower energies (~MeV) yield much lower rates of damage accumulation and thus less extensive structural modification. At a fluence of 2.5×10^{15} ions/cm^2, only the initial stages of the cubic-to-monoclinic (C to B) phase transformation process, consisting of the formation and aggregation of defects, have been observed. *Published by AIP Publishing.*
https://doi.org/10.1063/1.5013018

Lanthanide sesquioxides, Ln_2O_3 (Ln = La-Lu), have many applications, such as dielectrics,[1] ultrafast laser materials,[2] and neutron absorbers for nuclear energy systems.[3] They are also commonly studied as isostructural analogues of U_2N_3 and actinide sesquioxides, which are important nuclear fuel-related materials but are difficult to study directly.[4]

Most lanthanide sesquioxides (Sm_2O_3-Lu_2O_3) exhibit a cubic C-type ($Ia\bar{3}$) structure, the bixbyite structure, under ambient conditions.[4] Five distinct polymorphs can be formed under high temperature and high pressure conditions.[4] The complex high temperature and pressure polymorphism results from the many accessible transformation pathways in the lanthanide sesquioxides.[5]

The response of lanthanide sesquioxides to irradiation has previously been studied using ions with various energies: 30 keV O (<2 keV/u);[6] 300 keV Kr (<5 keV/u);[7–12] and swift heavy ions (185 MeV Xe and 2.2 GeV Au, $>10^4$ keV/u).[13,14] Irradiation-induced crystalline-to-crystalline structural transitions, from C-type bixbyite structures ($Ia\bar{3}$) to B-type monoclinic ($C2/m$) or A-type hexagonal ($P6_3/mmc$) polymorphs or even to another non-equilibrium X-type cubic ($Im\bar{3}m$) phase, have been observed.[6–15] Similar irradiation-induced phase transformations have been observed in isostructural Y_2O_3.[16–18] The work by Tracy *et al.*[13] on the response of these materials to swift heavy ion irradiation has demonstrated that the specific phase transformation induced by irradiation depends strongly on two factors: (*i*) the density of energy deposition from ion irradiation and (*ii*) the ionic radii of the constituent lanthanide elements. This is consistent with the results from ion irradiations in a broad range of energies (30 keV to 2.2 GeV),[6–15] all of which show similar energy and cation species dependencies.

Lanthanide sesquioxides of intermediate mass tend to transform to the monoclinic B-type phase under irradiation,[6–12,15] whereas the heaviest lanthanides can transform to the X-type phase.[13] Regardless of the specific transformation induced, the propensity of lanthanide sesquioxides to undergo an irradiation-induced phase transformation decreases across the lanthanide series (from Nd to Lu) due to factors like decreasing ionic radius and increasing ⟨Ln-O⟩ bond covalency.[19,20] Among all the irradiation-induced phase transformations, the cubic-to-monoclinic transformation is the most commonly reported, while C to X has been observed for only a few compositions (Tm_2O_3 and Lu_2O_3).[13]

In the work of Tracy *et al.*,[13] a model for the irradiation-induced cubic-to-monoclinic transformation mechanism, derived from the work of Hyde on redox-driven phase transformations,[21] was developed. The irradiation-induced production of anti-Frenkel defects (anion interstitial-vacancy pairs) leads to the aggregation of anion vacancies into planar clusters. These vacancy-type dislocation loops result in crystallographic shear of adjacent cation planes, triggering the local rearrangement of cations into the monoclinic structure. This monoclinic region expands with further irradiation-induced anion displacements. Although the cubic-to-monoclinic transformation has been studied in detail, the initial stage of defect formation that drives the transformation has not been directly observed and characterized.

In this work, the nanoscale changes that result from ion irradiation (using 1 MeV Kr ions) of two lanthanide sesquioxides, Gd_2O_3 and Lu_2O_3, were investigated. Gd_2O_3 represents sesquioxides with relatively large (r_{Gd} = 107.8 pm), light lanthanide cations that readily transform under irradiation, while Lu_2O_3 represents those with a smaller ion radius (r_{Lu} = 100.1 pm) that are typically more resistant to transformation. Ion irradiation combined with *in situ* transmission electron microscopy (TEM) observation and electron diffraction

a)cchen19@stanford.edu

was performed. Ion irradiation-induced behavior was investigated at room temperature and cryogenic temperature (120 K), in order to observe the initial stages of structural change and to determine the initial mechanisms of defect formation and aggregation prior to the phase transition. The early stages of defect formation that yield the cubic-to-monoclinic phase transformation were directly observed in Gd_2O_3 at 120 K, while neither material exhibited similar defect accumulation at room temperature.

Powder samples of Gd_2O_3 and Lu_2O_3 with typical grain sizes from 300 to 1000 nm were purchased from Alfa Aesar. To ensure crystallinity and to remove any residual water, the powders were annealed in air for 24 h at 1000 K. Both materials were confirmed to exhibit the cubic, C-type structure prior to irradiation and imaging. Before irradiation, Gd_2O_3 and Lu_2O_3 powders were dispersed onto TEM carbon grids. For each specimen, the thin region on the edge of each particle provided ideal high-resolution imaging conditions.

Irradiation was performed using the IVEM-Tandem facility in the Electron Microscopy Center (EMC) at Argonne National Laboratory.[22] The samples were loaded into a Hitachi-9000 NARTEM, equipped with a side-entry Gatan liquid helium (L_{He}) cooling stage and an incident ion beam at 30° from the microscope optic axis. TEM specimens were irradiated separately at room temperature and 120 K using 1 MeV Kr ions up to a total dose of 10^{16} ions/cm^2. The flux for Kr^+ irradiations was controlled at 2.5×10^{11} ions/cm^{2}s. Measurements were performed every 2.5 dpa (1.25×10^{15} ions/cm^2). Conditions were selected for comparison with previous work.[7–12] Because the structural stability of sesquioxides with small, heavy lanthanide cations (e.g., Lu_2O_3) has already been demonstrated under irradiation at cryogenic temperature,[8] only Gd_2O_3 was investigated at these low temperature conditions in the current work. Irradiation parameters were calculated using the SRIM 2012 code[23] assuming a default displacement energy of 25 eV for both Gd and Lu and an oxygen displacement energy of 28 eV.

Following irradiation of Gd_2O_3 to the maximum fluence of 2.5×10^{15} Kr/cm^2 (5 dpa) at 120 K, post-irradiation TEM examinations were carried out on two microscopes: an FEI Tecnei TEM and an FEI Titan. A negative spherical aberration imaging (NCSI) technique, which is beneficial to study simultaneously the details of the cation and the oxygen sublattices,[24] was used on the FEI Titan. By applying a negative value of the spherical-aberration coefficient of the objective lens under the imaging mode with a slight defocus condition (about $C_s = -40\ \mu$m and $Z = 10$ nm), the oxygen atom columns could be imaged and the contrast could be enhanced with overcompensation of spherical aberration.[25,26] All TEM observations were performed with a 300 kV accelerating voltage.

The unirradiated Gd_2O_3 and Lu_2O_3 powder specimens exhibited a well-crystallized cubic, C-type structure.[13] The observed structure is in agreement with the phase diagram, as this cubic (C-type) structure is the most stable phase at room temperature for lanthanide sesquioxides with cations of atomic number higher than that of Pm ($Z = 61$).

At room temperature, the initial cubic crystal structures of both Lu_2O_3 and Gd_2O_3 were maintained following irradiation with 1 MeV Kr ions up to a dose of 20 dpa. As illustrated in Fig. 1(b), the diffraction rings of polycrystalline Lu_2O_3 remained as the irradiation dose increased. The absence of diffuse scattering bands indicates that amorphization did not occur, and no rings corresponding to another structure emerged. Gd_2O_3 exhibited similar structural stability, which can be inferred from the results of the microdiffraction patterns after tilting, as illustrated in Fig. 1(d). The electron beam was placed on small grains that were then tilted close

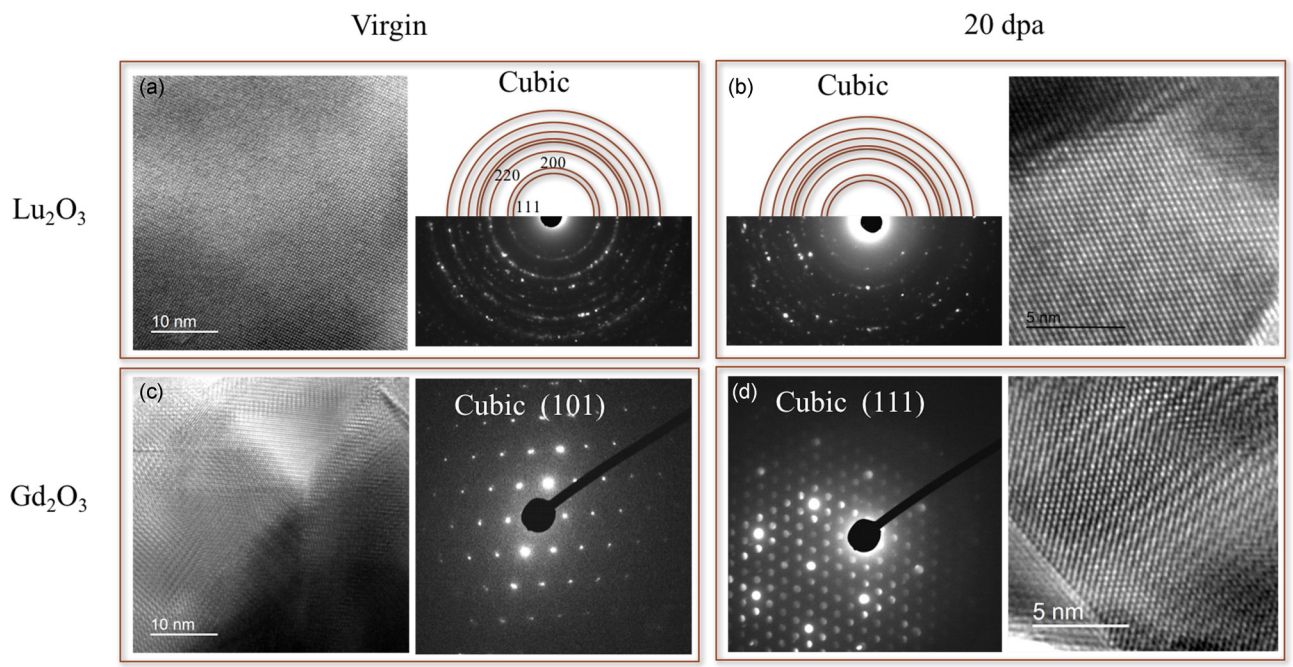

FIG. 1. The bright-field images and corresponding electron diffraction patterns of un-irradiated and irradiated Lu_2O_3 and Gd_2O_3. With an irradiation dose up to 20 dpa, the structure of polycrystalline Lu_2O_3 is retained [as illustrated by the ring pattern in (b)]. The same is true for Gd_2O_3, for which the cubic structure can be indexed after tilting (d). Dislocations or other defects are not observed from the bright-field images, indicating that the material has fully retained its crystallinity.

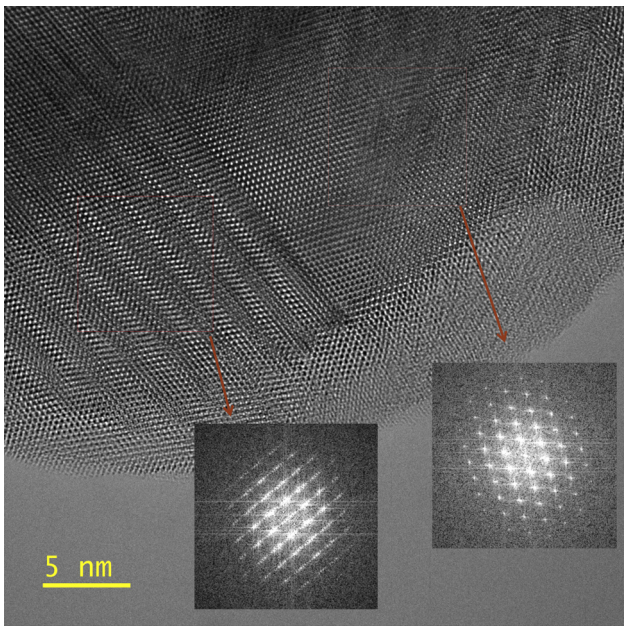

FIG. 2. High-resolution TEM image of Gd_2O_3 irradiated with 1 MeV Kr ions to a fluence of 2.5×10^{15} Kr/cm^2 (5 dpa) at 120 K. An irradiation-induced stacking fault layer structure is observed on the left side of the image. Also shown as insets are fast Fourier transforms (FFTs) from the regions of the original and stacking fault structure in the high-resolution TEM image. These FFTs were obtained with the ⟨210⟩ zone axis of the cubic Gd_2O_3 parallel to the electron beam direction.

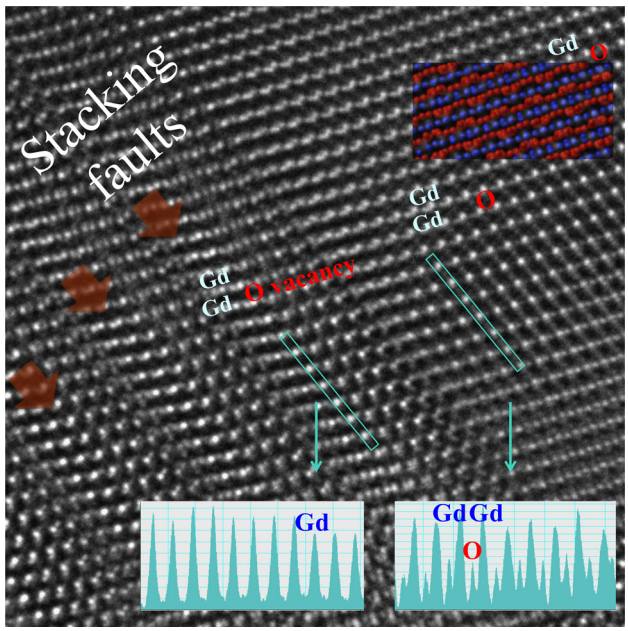

FIG. 3. Negative C_s corrected High-resolution TEM image of the irradiation-induced stacking fault layer structure. The structure is projected along the ⟨210⟩. Atom columns of Gd appear bright on a dark background, and dimmer oxygen columns are atomically resolved between the Gd layers. In the upper right inset, the anion (O) is labeled in red and cation (Gd) is labeled in blue, as simulated using the software CrystalMaker. A low oxygen occupancy is observed in the stacking fault layers (as indicated by the orange arrows). As directly resolved from the intensity scans (bottom insets) through the Gd-O column, an extremely low oxygen occupancy in the stacking fault layers is resolved.

to the low index directions to resolve their diffraction patterns. As shown in Figs. 1(b) and 1(d), clear lattice fringes are apparent in the bright field TEM image of the Lu_2O_3 and Gd_2O_3 after 20 dpa irradiation. There is no evidence of the formation of amorphous domains or of dislocations as nanoscale defects.

At 120 K, no obvious phase transformation could be observed from the bright field images and electron diffraction patterns of Gd_2O_3 above 5 dpa. In contrast, an obvious structural change was observed in the HRTEM images. Under negative spherical aberration imaging, a newly formed stacking fault structural feature, which exhibits periodicity related to that of the monoclinic structure seen from the ⟨001⟩ direction, was clearly resolved (Fig. 2).

The stacking fault structure was formed along the ⟨001⟩ direction of the initial Gd_2O_3 cubic structure, suggesting that a rearrangement of cations (Gd) was induced by atomic displacement at low temperatures. With overcompensation of the objective-lens aberration, as shown in the high resolution image in Fig. 3, anions (O) and cations (Gd) can both be resolved with a reduced signal strength (dimmer spot) and increased signal strength (brighter spot), respectively. The contrast changes dramatically between the stacking fault region and the surrounding stacking fault-free region. The spots corresponding to atomic columns of O become very dim or absent in the periodically spaced planes of the stacking fault region, suggesting that planar O vacancy clusters have formed. Viewing from the ⟨210⟩ direction, the stacking fault structure can be understood as a region containing a high concentration of oriented, planar O vacancy clusters, which induced a structural shear to move the adjacent cation planes to their new position and form the stacking faults. This newly formed stacking fault structure is an anion vacancy-dominated phase, which is consistent with the initial stages of the cubic-to-monoclinic transformation mechanism.[13]

Defect formation/accumulation did not occur in response to room temperature irradiation of these Ln_2O_3 compounds with 1 MeV Kr, in contrast to swift heavy ion irradiation which induced amorphization and/or phase transformations at this temperature depending on the type of ion and ion energy.[13] In the absence of these defects, formed by more extreme energy deposition, the original cubic crystal structure was retained in the current study. This is in agreement with previous studies of similar ion irradiation conditions (mass and energy).[7–12] No susceptibility of several lanthanide sesquioxides to amorphization or extensive defect formation has been demonstrated under room temperature irradiation at similar energies.[7–12] In contrast, at 120 K, Dy_2O_3 exhibited a transformation path as illustrated below (1), while Er_2O_3 and Lu_2O_3 showed less or no susceptibility to a radiation-induced phase transformation[7–12]

$$\text{Cubic, C}-\text{type}\,(Ia\bar{3}) \xrightarrow{2.5\,dpa} \text{disordered fluorite} \xrightarrow{5\,dpa} \text{Monoclinic, B}-\text{type}\,(C2/m) \xrightarrow{25\,dpa} \text{Hexagonal, H}-\text{type}\,(P63/mmc). \quad (1)$$

These results reveal a clear inverse relation between the lanthanide atomic number and propensity to undergo a phase transformation, as well as an inverse relation between irradiation temperature and the propensity to undergo a phase transformation. Tang *et al*. have suggested that the irradiation dose dependence of this cubic-to-monoclinic phase transformation is directly related to the temperature of the cubic/monoclinic phase boundary in the Ln_2O_3 phase diagram.[9] As a result, the threshold dose that triggers this transformation is higher in Dy_2O_3 than in Er_2O_3, just as is the thermal energy necessary to trigger the transformation at the phase boundary at elevated temperatures. In addition, the transformation rate decreases as lanthanides of smaller ionic radii are substituted into the structure. This is consistent with our experimental results, wherein both trends (compositional dependence of transformation dose and rate) are confirmed. Similar irradiation behavior under swift heavy ion irradiation has been reported,[13] wherein the compounds with a smaller lanthanide atomic number (e.g., Sm_2O_3) are more susceptible to irradiation-induced phase transformations. For compounds with a larger lanthanide atomic number (Tm_2O_3 and Lu_2O_3), phase transformations were, at a given fluence, less extensive under ion irradiation, even in response to very dense electronic excitation.

This compositional trend is consistent with the compositional variation of many material properties across the lanthanide series, such as the increased ⟨Ln-O⟩ bond covalency[19,20] and increased cubic-to-monoclinic phase transition enthalpy[27] with increasing lanthanide atomic number. As a result, breaking ⟨Ln-O⟩ bonds and inducing the formation of point defects is difficult for lanthanide sesquioxides with a high atomic number. This explains why irradiation induced phase transformations are often observed only for Ln_2O_3 materials with a smaller atomic number, as seen in the current results.

Based on the TEM and XRD results of Tang *et al*.,[7–12] an irradiation-induced phase transition can be expected in Gd_2O_3 due to its relatively large cation radius (as compared with Dy_2O_3 and Er_2O_3, for which the initial monoclinic phase formed after exposure to doses of around 5 and 17 dpa, respectively). However, different from the results of irradiated bulk Er_2O_3,[7–12] *in situ* irradiation using 1 MeV Kr did not induce a complete phase transition in Gd_2O_3 up to 5 dpa. This might be due to the absence of the compressive biaxial stresses[9] that occur in bulk materials and influence their responses to irradiation. When thin TEM samples are irradiated, point defects can be efficiently annihilated at the surfaces of the thin foils, leaving fewer defects available to induce structural modification as compared with irradiation of bulk materials.[9]

Therefore, even with larger cation ionic radii ($r_{Gd} > r_{Er}$) and a dose (5 dpa) above the critical value to trigger a phase transition in Er_2O_3 (2.5 dpa), no phase transformation was observed.

As illustrated in Fig. 3, the early stages of structural change are driven by defect accumulation under irradiation, suggesting that once displacement-induced oxygen vacancies are formed, vacancy aggregation will be the most crucial process in the initial stage of the phase transformation. The migration energy of oxygen vacancies in this material is approximately 1 eV, making anion vacancies the most mobile defects in the cubic phase.[28,29] Prior work has also shown that the diffusion rate of oxygen vacancies is 10^5–10^6 times faster than that of the cations,[30] such that they can assemble into the planar vacancy clusters that then induce cation rearrangement through the resulting shear of adjacent cation planes.

The observation of stacking disorder and ordered planar anion vacancy clusters is in good agreement with the transformation mechanism reported by Tracy *et al*.,[13] based on the work of Hyde.[21] In this model, the oriented planar anion vacancy clusters facilitate crystallographic shear of adjacent anion planes, prompting the phase transformation. The lack of a complete transformation in the present work may be due to the need for higher ion fluences, and therefore higher produced defect concentrations, to initiate formation of the monoclinic phase. Still, the NCSI technique provides direct evidence that irradiation-induced anion vacancies tend to form periodically spaced planar clusters in the lanthanide sesquioxides following irradiation and that this yields modification of adjacent cation planes.

This finding is in agreement with simulation studies by Fabris *et al*. of structurally related yttrium-stabilized zirconia (YSZ), showing that the relaxation of atoms adjacent to anion vacancies in fluorite structured materials can lead to structural distortion, resulting in a distinct short-range atomic structure with non-cubic symmetry.[31] It is further known from the XRD study of YSZ that critical oxygen vacancy concentrations are essential to stabilize the cubic, tetragonal, and monoclinic phases,[32] indicating the role of these defects in phase transformations. Sufficient vacancy concentration production will lead to a phase transformation by aggregation and corresponding collective local atomic rearrangement, as with the previously described anion vacancy-driven cubic-to-monoclinic transformation mechanism in the lanthanide sesquioxides.

Because of the critical role that oxygen vacancies play in this transformation mechanism, it is essential to understand the special orientation and the correlation between the original lattice structure and these oxygen defects. Lacroix *et al*.[33] have demonstrated that oxygen vacancy dislocation loop formation is energetically favorable in the (222) anion plane of bixbyite-structured Y_2O_3 (isostructural with the cubic lanthanide sesquioxides) under ion beam processing, suggesting that these sites will preferentially accommodate anion vacancies.

In this work, although vacancy loops in the (222) planes cannot be observed in Gd_2O_3 from the ⟨210⟩ direction, an anion displacement driven structural change (a partially altered periodicity) is found on the Gd (002) plane. The early stage of ion irradiation-induced crystalline-to-crystalline phase transformations is observed in the form of a local anion vacancy formation dominated structural modification process.

In summary, *in situ* and *ex situ* TEM observations of the structural modification of lanthanide sesquioxides Gd_2O_3 and Lu_2O_3 after ion irradiation with 1 MeV Kr ions were performed. The initial cubic structures of both materials were retained up to a dose of 20 dpa at room temperature. However, at 120 K, stacking fault and planar anion vacancy cluster formation were observed in Gd_2O_3. This structural modification is identified as the initial stage of the known

irradiation-induced, cubic-to-monoclinic phase transformation, which proceeds *via* a mechanism driven by the production and aggregation of anion vacancies.

This research was supported as part of the Energy Frontier Research Center Materials Science of Actinides, an Energy Frontier Research Center funded by the U.S. Department of Energy, Office of Science, Basic Energy Sciences under Award No. DE-SC0001089. Part of this work was performed at the Stanford Nano Shared Facilities (SNSF). The electron microscopy with in situ ion irradiation performed at the IVEM-Tandem Facility, Argonne National Laboratory was supported by the U.S. Department of Energy, Office of Nuclear Energy under DOE Idaho Operations Office Contract DE-AC07- 051D14517 as part of a Nuclear Science User Facilities experiment. C.-H.C. is grateful to M. Li, M. A. Kirk, P. M. Baldo, J. Hu, and E. A. Ryan for their assistance with the IVEM experiments. C.-H.C. is also grateful to A. L. Koh for the assistance of the NCSI technique.

[1]M. Hong, J. Kwo, A. R. Kortan, J. P. Mannaerts, and A. M. Sergent, Science **283**, 1897 (1999).
[2]A. A. Kaminskii, S. N. Bagaev, H. J. Eichler, K. Ueda, K. Takaichi, A. Shirakawa, H. Yagi, T. Yanagitani, and H. Rhee, Laser Phys. Lett. **3**, 310 (2006).
[3]M. Durazzo, F. B. V. Oliveira, E. F. Urano de Carvalho, and H. G. Riella, J. Nucl. Mater. **400**, 183 (2010).
[4]R. D. Baybarz, J. Inorg. Nucl. Chem. **35**, 4149 (1973).
[5]G-y. Adachi and N. Imanaka, Chem. Rev. **98**, 1479 (1998).
[6]B. Antic, A. Kremenovic, I. Draganic, P. Colomban, D. Vasiljevic-Radovic, J. Blanusa, M. Tadic, and M. Mitric, Appl. Surf. Sci. **255**, 7601 (2015).
[7]M. Tang, J. A. Valdez, K. E. Sickafus, and P. Lu, JOM **59**, 36 (2007).
[8]M. Tang, P. Lu, J. A. Valdez, C. R. Stanek, and K. E. Sickafus, Phys. Status Solidi (c) **4**, 1171 (2007).
[9]M. Tang, P. Lu, J. A. Valdez, and K. E. Sickafus, J. Appl. Phys. **99**, 063514 (2006).
[10]M. Tang, P. Lu, J. A. Valdez, and K. E. Sickafus, Philos. Mag. **86**, 1597 (2006).
[11]M. Tang, P. Lu, J. A. Valdez, and K. E. Sickafus, Nucl. Instrum. Methods B **250**, 142 (2006).
[12]M. Tang, J. A. Valdez, P. Lu, G. E. Gosnell, C. J. Wetteland, and K. E. Sickafus, J. Nucl. Mater. **328**, 71 (2004).
[13]C. L. Tracy, M. Lang, F. Zhang, C. Trautmann, and R. C. Ewing, Phys. Rev. B **92**, 174101 (2015).
[14]M. Lang, F. Zhang, J. Zhang, C. L. Tracy, A. B. Cusick, J. VonEhr, Z. Chen, C. Trautmann, and R. C. Ewing, Nucl. Instrum. Methods B **326**, 121 (2014).
[15]G. Sattonnay, S. Bilgen, L. Thomé, C. Grygiel, I. Monnet, O. Plantevin, C. Huet, S. Miro, and P. Simon, Phys. Status Solidi B **253**, 2110 (2016).
[16]R. J. Gaboriaud, B. Lacroix, and F. Paumier, Nucl. Instrum. Methods B **277**, 18 (2012).
[17]R. J. Gaboriaud, F. Paumier, M. Jublot, and B. Lacroix, Nucl. Instrum. Methods B **311**, 86 (2013).
[18]R. Gaboriaud, F. Paumier, and B. Lacroix, Nucl. Instrum. Methods B **327**, 44 (2014).
[19]M. Rahm and N. V. Skorodumova, Phys. Rev. B **80**, 104105 (2009).
[20]M. V. Ryzhkov, V. A. Gubanov, Y. A. Teterin, and A. S. Baev, Condens. Matter **59**, 7 (1985).
[21]B. G. Hyde, Acta Cryst. **27**, 617 (1971).
[22]See www.ne.anl.gov/ivem/ for "Intermediate voltage electron microscopy (IVEM)-tandem facility," Argonne National Laboratory.
[23]J. F. Ziegler, M. D. Ziegler, and J. P. Biersack, Nucl. Instrum. Methods B **268**, 1818 (2010).
[24]K. W. Urban, C. L. Jia, L. Houben, M. Lentzen, S. B. Mi, and K. Tillmann, Philos. Trans. R. Soc. **367**, 3735 (2009).
[25]C. L. Jia, M. Lentzen, and K. Urban, Microsc. Microanal. **10**, 174 (2004).
[26]C. L. Jia, M. Lentzen, and K. Urban, Science **299**, 870 (2003).
[27]M. Zinkevich, Prog. Mater. Sci. **52**, 597 (2007).
[28]L. Kittiratanawasin, R. Smith, B. P. Uberuaga, and K. E. Sickafus, J. Phys. Condens. Matter **21**, 115403 (2009).
[29]L. Kittiratanawasin, R. Smith, B. P. Uberuaga, K. E. Sickafus, A. R. Cleave, and R. W. Grimes, Nucl. Instrum. Methods B **266**, 2691 (2008).
[30]T. H. Etsell and S. N. Flengas, Chem. Rev. **70**, 339 (1969).
[31]S. Fabris, A. T. Paxton, and M. W. Finnis, Acta Mater. **50**, 5171 (2002).
[32]P. Kountouros and G. Petzow, *Defect Chemistry, Phase Stability and Properties of Zirconia Polycrystals* (Technomic, Lancaster, Basel, 1993).
[33]B. Lacroix, F. Paumier, and R. J. Gaboriaud, Phys. Rev. B **84**, 014104 (2011).